Composites Science and Technology 68 (2008) 3322–3329

Contents lists available at ScienceDirect

Composites Science and Technology

journal homepage: www.elsevier.com/locate/compscitech

Electrospun nanofiber reinforced and toughened composites through in situ nano-interface formation

Song Lin [a], Qing Cai [a], Jianying Ji [a], Gang Sui [a], Yunhua Yu [a], Xiaoping Yang [a,*], Qi. Ma [b], Yan Wei [b], Xuliang Deng [b,*]

[a] The Key Laboratory of Beijing City on Preparation and Processing of Novel Polymer, Beijing University of Chemical Technology, Beijing 100029, China
[b] School and Hospital of Stomatology, Peking University, Beijing 100081, China

ARTICLE INFO

Article history:
Received 17 January 2008
Received in revised form 20 August 2008
Accepted 29 August 2008
Available online 18 September 2008

Keywords:
B Interface
A Fiber
A Nano-composite

ABSTRACT

PAN core–PMMA shell nanofiber fabric was prepared by electrospinning of polymer blends to reinforce 2,2-bis-[4-(methacryloxypropoxy)-phenyl]-propane (Bis-GMA) a dental resin system. The core–shell structure of the PAN–PMMA nanofiber was confirmed by scanning electron microscopy (SEM) and transmission electron microscope/energy dispersive spectroscopy (TEM/EDS) observation. The flexural properties and dynamic mechanical properties of the PAN–PMMA nanofiber reinforced Bis-GMA composites were studied. Results showed that PMMA shell was partly dissolved with the Bis-GMA resin. After photopolymerization, liner PMMA chains interpenetrated and entangled with the dental resin network, which resulted in an in situ nano-interface in the shell structure. Improvement of the mechanical properties of the PAN–PMMA nanofiber reinforced Bis-GMA composites has been achieved through this nano-interface formation.

1. Introduction

The advanced dental composite research is focus on producing a material that have perfect filler–resin interface and present high strength and toughness properties, which can be used in all circumstances [1,2]. The major work on dental restoration composites is center on short glass fibers, silica or glass particles or whisker reinforcements for improving mechanical properties [3–6]. But these fillers are not strong enough or may create stress concentration points throughout the matrix caused by their irregular shapes, and then composites exhibit cracks that either cut through the fillers or propagate around the filler particles [7]. Nanometer-sized fillers are widely believed to have the potential to substantially improve polymer mechanical properties at very low filler loadings, for their large interfacial area enables the applied load to be transferred on filler–matrix interface [8]. However, failure often occurred when the composite materials were subjected to longer time usage. One major reason proposed for this failure is the poor adhesion between the fillers and polymer matrix. Good bonding between fillers and the resin matrix is essential in composites to improve their mechanical and physical properties [9–11]. Strong adhesion is the prerequisite for transferring load sufficiently from matrix to either nanofibers or nanoparticles with high surface areas [12–14]. Silanation is commonly used to promote dental resin matrix–nanofiller adhesion [7,15], but silane coupling agents tend to form aggregates on the filler surface resulting in an unstable bond between fillers and resin, and this bond can be degraded by water absorbed by the composites [16]. So in this field, dental composites do not have enough toughness, strength and durability in order to be used in stress bearing areas [17].

So far, polymer nanofibers made from electrospinning have been much less used as composite reinforcements. Only limited researchers have tried to make nanocomposites reinforced with electrospun polymer nanofibers [18–21]. Among them, Fong et al. [18,19] had ever used electrospun Nylon 6 to reinforce the dental methacrylate of Bis-GMA/TEGDMA, and theirs results indicated flexural strength (FS), elastic modulus (E_Y) and work of fracture (WOF) of the nanofiber reinforced composite resins were all increased with relatively small amounts of Nylon 6 nanofibers. However, there were two major drawbacks in their study to prevent further increasing mechanical properties. First, pullout of Nylon 6 nanofibers from matrix were observed during the three-point bending test, which indicated the interface between the fiber and the matrix still needed to be further improved. Secondly, the chief advantage of nylon lies in its resistance to shock and repeated stressing, which makes it good candidate reinforcement for dental composites. However, hydrophilicity of nylon could cause water absorption and thus affects the mechanical properties of nylon nanofibers themselves and corresponded composites thereof.

Some core–shell fibers, such as poly (methyl methacrylate) (PMMA)–polyacrylonitrile (PAN), PMMA–polystyrene (PS), Polybu-

* Corresponding authors. Tel./fax: +86 10 64412084 (X. Yang); tel.: +86 10 62173403 (X. Deng).
E-mail addresses: yangxp@mail.buct.edu.cn (X. Yang), kqdxl@bjmu.edu.cn (X. Deng).

0266-3538/$ - see front matter © 2008 Elsevier Ltd. All rights reserved.
doi:10.1016/j.compscitech.2008.08.033

tadiene (PB)–PS, PAN–PMMA and nylon–PMMA fibers, had been reported in recent years [22–26]. These fibers were made either by coaxial-electrospinning with coannular nozzles [25,26] or by co-electrospinning polymer blends using a single-nozzle technique. Usually, good concentricity is hard to be achieved in coaxial-electrospinning, while excellent core–sheath structure had been identified by using the latter technique [22–24]. It was found that the formation of core–sheath structures in polymer blends electrospinning depended strongly on factors including difference in polymer solubility parameters, molecular mobility and solvent evaporation rate, etc. Theoretically, such core–shell nanofibers which is designed to have a core with high strength and a shell to provide good adhesion with resin matrix through chemical bonding or formation of IPN structure, will submit a kind of novel nanocomposite possessing of excellent mechanical properties. However, no report has been published on using core–shell electrospun nanofibers to reinforce dental resin.

Accordingly, this study reports the preparation of PAN core–PMMA shell structured nanofibers by co-electrospinning of polymer blends and the application of the nanofibers to reinforce Bis-GMA dental resin system. PMMA shell can partly dissolved in Bis-GMA resin, and a semi-IPN structure will form after Bis-GMA being photopolymerized to remarkably improve the interfacial properties between fibers and matrix, which had been proved to be a effective method to ameliorate the adhesion of glass fiber to Bis-GMA matrix [27,28]. To obtain this purpose, (i) PAN core–PMMA shell structured nanofiber was electronspun, (ii) nanofiber reinforced composites were fabricated, and (iii) flexible properties and dynamic mechanical properties of the nano-composites were investigated, in order to clarify the characterization of in situ interfacial interaction between core-shell nanofibers and Bis-GMA resin.

2. Materials and methods

2.1. Materials

Commercial PAN fibers composed of PAN/methyl acrylate/itaconic acid (93:5.3:1.7 w/w, M_W = 100,000 g/mol, Courtaulds Ltd., UK) and PMMA particles (M_W = 500,000 g/mol, LG Ltd., Korea) were purchased for electrospinning core–shell structure nanofibers. Dimethylformamide (DMF, solvent), Bis-GMA resin, tri-(ethylene glycol) dimethacrylate (TEGDMA, diluter), camphorquinone (CQ, photo-initiator), and 2-(dimethylamino) ethyl methacrylate (DMAEMA, co-initiator) were supplied by Aldrich Chemical Co. Fig. 1 shows the molecular structures of resin and initiators used in the experiment.

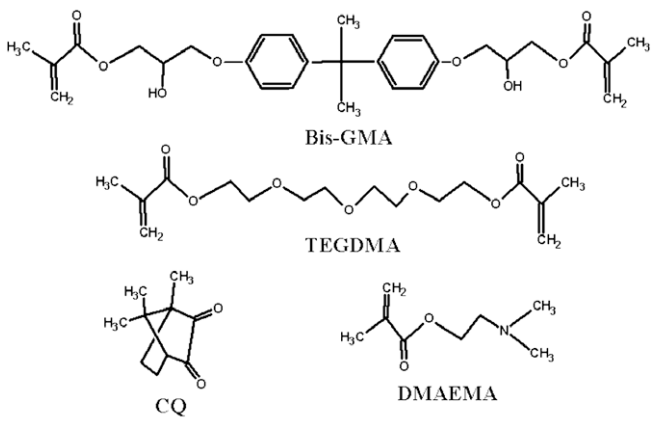

Fig. 1. Molecular structures of dental monomers and initiators.

2.2. Electrospinning of PAN core–PMMA shell nanofibers

1.8 g PAN fibers and 0.6 g PMMA particles were dissolved in 10 ml dimethylformamide (DMF), respectively, which were mixed together and stirred magnetically for about 3 h to obtain a homogeneous solution [A]. 1.2 g PAN fibers [B] and 1.2 g PMMA particles [C] were also dissolved in 10 ml DMF, respectively. The shear viscosity of all solutions was measured by using a digital rotation viscometer (NDJ-5S, China) under the same shear rate about 400 s^{-1}.

All solutions were electrospun in the same condition. These solutions were directly electrospun using a typical electrospinning equipment [29]. The solution was fed to the 5 ml needle tip (0.4 mm dia.) using a syringe pump (TOP 5300) at a 0.4 ml/h^{-1} flow rate. As the electrical field increased, nanofibers were spun and collected on a grounded metal sheet with 10 cm width and 15 cm length. The applied voltage (DW-P303-1AC, China) was kept at 16 kV, and the distance between the needle tip and the metal sheet was 17 cm. All the nonwoven fabrics were dried in a vacuum oven at 60 °C for 48 h, which were approximately 7 mg/cm^2 in weight and 35 μm in thickness.

2.3. Fabrication of nanofiber reinforced composites

The nonwoven nanofibers fabrics were carefully cut into pieces with the size of 45 mm × 5 mm for DMTA test and 25 mm × 2 mm for three - point bending test. Teflon mold was used to produce 45 mm × 5.0 mm × 2.0 mm and 25 mm × 2.0 mm × 2.0 mm beam shape composite specimens. The nanofiber nonwoven fabrics pieces were laminated into the matrix layer by layer. Firstly, nonwoven nanofiber fabrics were carefully laid up into the mold. Then Bis-GMA/TEGDMA resin (50/50 wt%) with photo initiator CQ (mass fraction of 0.5%) and co-initiator DMAEMA (mass fraction of 1%) were poured into the mold to immerse with the fabrics. Vacuum oven was employed to remove the trapped air bubbles in the immersed pieces for about 24 h. All the specimens were photo-cured for 1 min using curing light (QHL 75 Densply) in the yellow-light room to avoid the premature curing, and stored at 37 °C for 48 h. The sides of the specimens were carefully polished with 2400 grit silicon carbide paper before tests. The final dimensions of the specimens were measured by vernier caliper.

2.4. Analysis and characterization

2.4.1. Core–shell structures

The morphologies of PMMA, PAN and PAN–PMMA nanofibers were observed by SEM (FESEM Hitachi S-4700). Based on the SEM photos, diameter range of the nanofibers was obtained by using image visualization software Image J. All the samples were sputter coated with a thin layer of gold to allow for better electrical conduction. A JEM-3010 TEM (JEOL Japan Inc.), operating at 300 kV with a measured point-to-point resolution of 0.17 nm and an energy dispersive X-ray spectroscopy (EDS) system (GENESIS 307, USA, EDAX, INC.), was used to identify and characterize the core-shell structure of the PAN–PMMA nanofibers. For the preparation of TEM samples, the nanofibers were, respectively, collected on two carbon-coated copper specimen grids during electrospining. Then one sample was dipped in acetone to dissolve the PMMA of the nanofiber. The elemental analysis of two nanofiber sample surfaces was carried out by EDS to determine nitrogen and oxygen element content.

2.4.2. Microstructure of in situ nano-interface

The flexural fracture surfaces of the nanofiber reinforced composite specimens were examined by SEM to observe interfacial adhesion between the nanofibers and dental resin matrix. All the

samples were sputter coated with a thin layer of gold to allow for better electrical conduction.

2.4.3. Dynamic mechanical properties

Dynamic mechanical properties of samples were determined using a dynamic mechanical thermal analyzer (Rheometry Scientific DMTA V) in a three-bending mode at a frequency of 5 Hz and a scan rate of 5 °C/min within −50–250 °C temperature range. The dimensions of specimens were 2.0 mm × 5.0 mm × 45 mm.

2.4.4. Flexural properties

The flexural strength, flexural modulus and work of fracture of Bis-GMA resin, PMMA nanofiber reinforced Bis-GMA composites, PAN nanofiber reinforced composites, PAN–PMMA nanofiber reinforced composites were measured in a three-point bending test. The size of the specimens was 2 mm × 2 mm × 25 mm. A Lloyd material testing machine (model LRX; Lloyd Instruments, Fareham, England) was used for the three-point bending test according to the ISO 10477:92 standard with a span of 20 mm and a crosshead speed of 1.0 mm/min. The load-deflection curves were recorded with a PC computer software (Nexygen, Lloyd Instruments, Fareham, England). Flexural strength (S_f), flexural modulus (E_y) and work of fracture (WOF) were calculated from the following formulae:

$$S_f = 3Fl/2bh^2 \quad (1)$$

$$E_y = l^3F_1/4fbh^3 \quad (2)$$

$$\mathrm{WOF} = A/bh \quad (3)$$

where F is the applied load (N) at the highest point of load-deflection curve, l is the span length (20.0 mm), b is the width of the test specimen, and h is the thickness of the test specimens, F_1 is the load (N) at a venient point in the straight line portion of the trace, f is the deflection (mm) of the test specimen at load F_1. A in Joules (J) is the work done by the applied load to deflect and fracture the specimen, corresponding to the area under the load-deflection curve WOF is the work of fracture in J/m^2 or kJ/m^2. Eight specimens were tested for average.

3. Results and discussion

3.1. Electrospinning of PAN core–PMMA shell nanofibers

Fig. 2 shows the SEM images of electrospun PMMA, PAN and PAN–PMMA nanofibers, respectively. The diameter of PMMA nanofibers was in the range from 800 to 1200 nm, and PAN nanofibers from 200 to 400 nm, while the diameter of PAN–PMMA nanofibers was in the range from 200 to 500 nm, thinner than that of PMMA nanofibers.

Fig. 3(a) presents the TEM image of electrospun PAN–PMMA nanofiber. The PAN–PMMA nanofiber exhibited relatively uniform core–shell structure along the fiber axis, with an outer diameter about 290 nm and a wall thickness about 50 nm. When the nanofibers were treated with acetone, it presents a single phase structure and the diameter was reduced to 220 nm as shown in Fig. 3(b). From the figure, only the PMMA was dissolved by acetone, which was located in the shell. In order to identify the compositions of the two kinds of nanofiber surface, EDS measurements were performed and the results were shown in the Fig. 3. The EDS spectra data were listed in Table 1. EDS measurements detected substantial amounts of nitrogen and oxygen element on the nanofiber surface. Atomicity ratios of nitrogen to oxygen were different from two kinds of nanofiber surface, 1:1.8(a/a) of the core-shell structure nanofibers and 1:1 (a/a) of the nanofiber surface by acetone treatment. PAN polymer displays the same N/O atomicity ratio (1:1) to the core phase. Thus, for the hybrid core-shell structured nanofibers, PAN was located in the core phase, and PMMA was moved outside to form the shell phase. This is different from the PMMA(core)–PAN(shell) nanofibers prepared by Bazilevsky et al. [23], although the same polymer pair was used.

Wei et al. [24,30] reported that the molecular weight distribution and viscosity ratio of compositions were impact factors on the development of electrospinning core-shell structured nanofibers. They reported that the higher viscous component was always located at the center and lower viscous component located in the outside [30]. In this study, molecular weight of PAN was higher than that of PMMA, which indicated that PAN had longer molecular

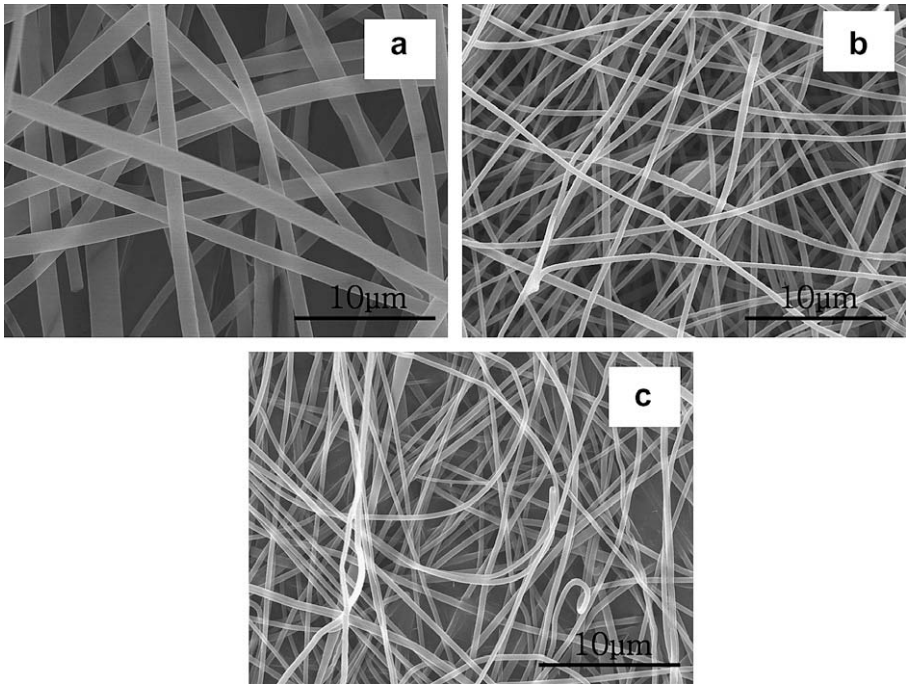

Fig. 2. SEM images of electrospun (a) PMMA nanofibers, (b) PAN nanofibers, and (c) PAN–PMMA nanofibers.

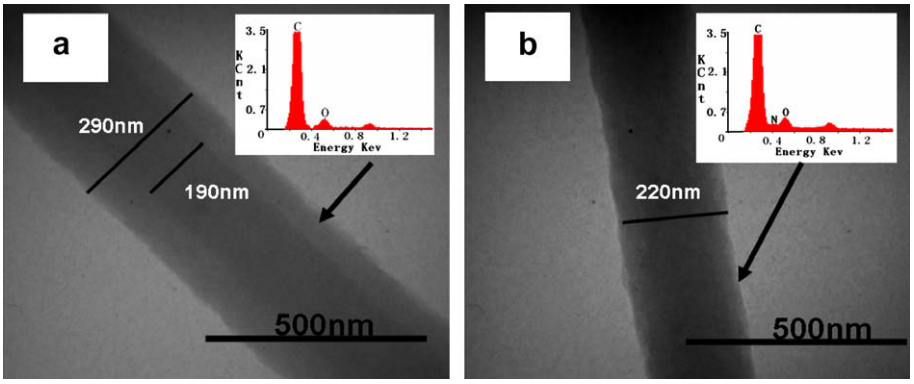

Fig. 3. TEM images and EDS measurement of PAN–PMMA nanofiber. (a) Untreated, (b) treated with acetone.

Table 1
EDS spectra data of PAN–PMMA nanofiber

sample	Element	Weight %	Atomic %	N:O (a/a)
Nanofiber treated with acetone	C	93.7	94.8	1:1
	N	2.9	2.6	
	O	3.4	2.6	
Untreated nanofiber	C	94.5	95.6	1:1.8
	N	1.8	1.6	
	O	3.7	2.8	

Table 2
Shear viscosity of PMMA, PAN and PAN–PMMA dissolved in DMF

	Polymer solution		
	PAN–PMMA (2.4 g/20 ml)[A]	PAN (1.8 g/10 ml)[B]	PMMA (0.6 g/10 ml)[C]
Viscosity (mPa.s)	400.6	798.4	11.3

chains than PMMA. In addition, the viscosity of PAN in the DMF solution was far higher than that of PMMA composition under the same shear rate, as shown in Table 2. Therefore, the short molecular chains endowed the PMMA molecules with high mobility to move outside to form the shell, while the PAN located inside to form the core. In Bazilevsky's report [23], however, their working fluid was a blend of PAN (M_w = 150 kDa) and PMMA (M_w = 996 kDa), which led to PMMA core–PAN shell nanofibers. In both cases, component separation was easily happened during electronspinning, which resulted in the production of core–shell structured nanofibers.

3.2. In situ nano-interface formation

Fig. 4 is the SEM images of the fracture surfaces of pure resin and the composites with 5 wt% and 7.5 wt% of PMMA nanofibers after three-point flexural testing. The fracture surface of 5 wt% PMMA nanofiber loaded composites was very rough, on which no

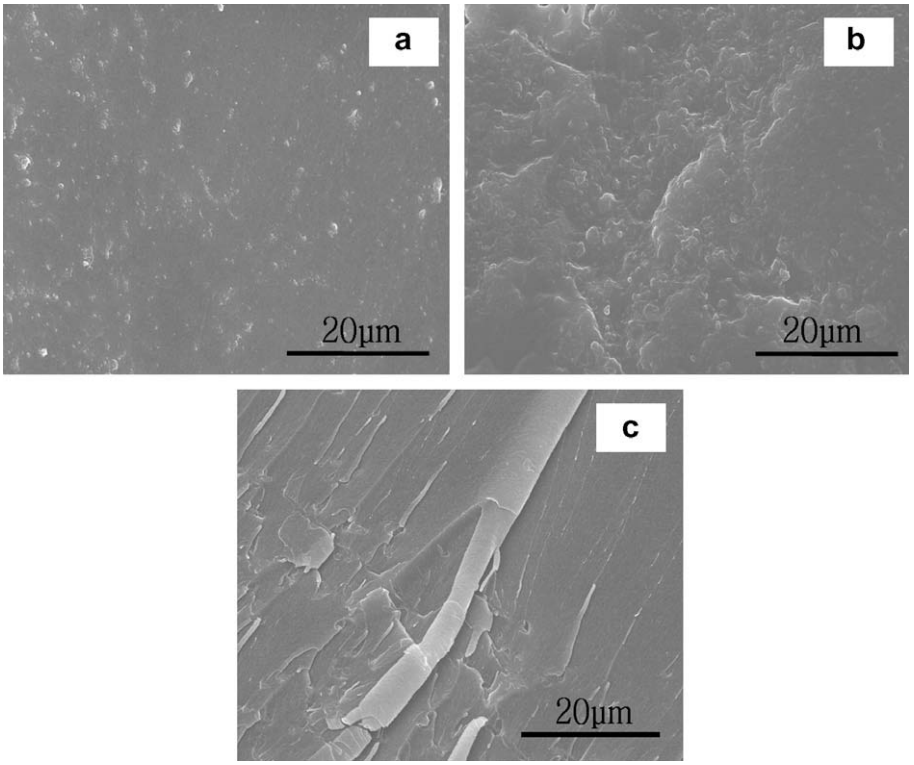

Fig. 4. SEM images of fracture surfaces. (a) Pure resin, (b) composite with 5 wt% PMMA nanofibers, and (c) 7.5 wt% PMMA nanofibers after three-point testing.

PMMA nanofibers were found. It was because that the methacryloyl groups on Bis-GMA main-chain could take favorable interaction with the methacryloyl groups on the side-chains of PMMA, and the PMMA nanofibers were partly dissolved into the dental monomers [27,28]. After photopolymerization, the linear PMMA could inter-penetrate and entangle with the cross-linked resin network to form a semi-IPN structure. However, when the PMMA content exceeded the dissolving capacity of dental monomers, some extra PMMA nanofibers were sticked together in the composites as shown in Fig. 4 (c).

Unlike PMMA nanofiber reinforced composites, both PAN and PAN–PMMA nanofiber kept fiber configuration in the composites (as shown in Fig. 5). However, distinguished difference was identified between the composites reinforced with PAN nanofibers and PAN–PMMA nanofibers by observing the fracture surfaces. For the PAN nanofiber reinforced composites, many pullout nanofibers were observed with little resin on the surface, which implied weak interfacial bonding between nanofibers and matrix. On the contrary, nanofibers in PAN–PMMA composites (Fig. 5a and b) were intimately adhered to the matrix on the fracture surfaces without visible apparent boundaries between nanofibers and matrix, indicating an enhanced interfacial bonding.

Just as PMMA nanofiber reinforced composites, PMMA located in the shell structure of the PAN–PMMA nanofibers could also form a semi-IPN structure with the dental resin. Therefore, an in situ nano-interface between the PAN–PMMA nanofibers and matrix was formed which resulted in good interfacial adhesion between the nanofibers and resin matrix.

In order to know the formation of in situ nano-interface clearly, a schematic representation on the formation of semi-IPN structure of the composites was presented, as seen in Fig. 6. When the PAN–PMMA nanofibers were immersed with the Bis-GMA/TEGDMA resin, PMMA located on the shell could dissolve with the Bis-GMA (Fig. 6b). After photopolymization, linear PMMA interpenetrated and entangled with the crosslinked dental resin network (Fig. 6c) and a semi-IPN structure was formed. It was reported that the interaction between polymer molecular chains and the surface of the nanofibers controls both the polymer molecular conformations at the surface and the entanglement distribution in a larger region surrounding the nanofibers [31–33]. For the PAN–PMMA nanofibers, PMMA located in the shell structure, with a large surface to volume ratio and just about 50 nm thicknesses can mostly dissolve in Bis-GMA as shown in Fig. 6b. After photopolymization, most of the PMMA chains entangled with the cross-linked dental resin network in a larger region surrounding the nanofibers (Fig. 6c), and a nano-interface was symmetrically and continuously formed between nanofibers and matrix, resulting in a flat configuration of the polymer on the surface of the nanofibers and a compact interface, as shown in Fig. 6d. Therefore, it is hard to find any pullout PAN–PMMA nanofibers on the fracture surface of the composites. The PAN–PMMA nanofiber composites not only introduce PMMA in the shell structure to improve the interfacial adhesion in the

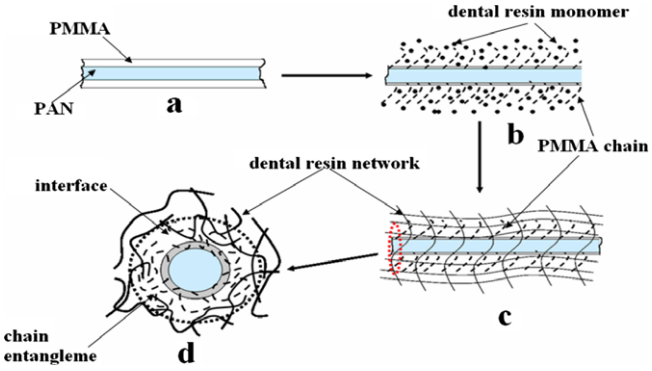

Fig. 6. Schematic representation of formation semi-IPN structure of the composite (a) PAN–PMMA nanofiber (b) PMMA shell of nanofibers dissolved with the dental resin (c) conform semi-IPN structure (d) chain entanglement of the interface to form in situ nano-interface interaction.

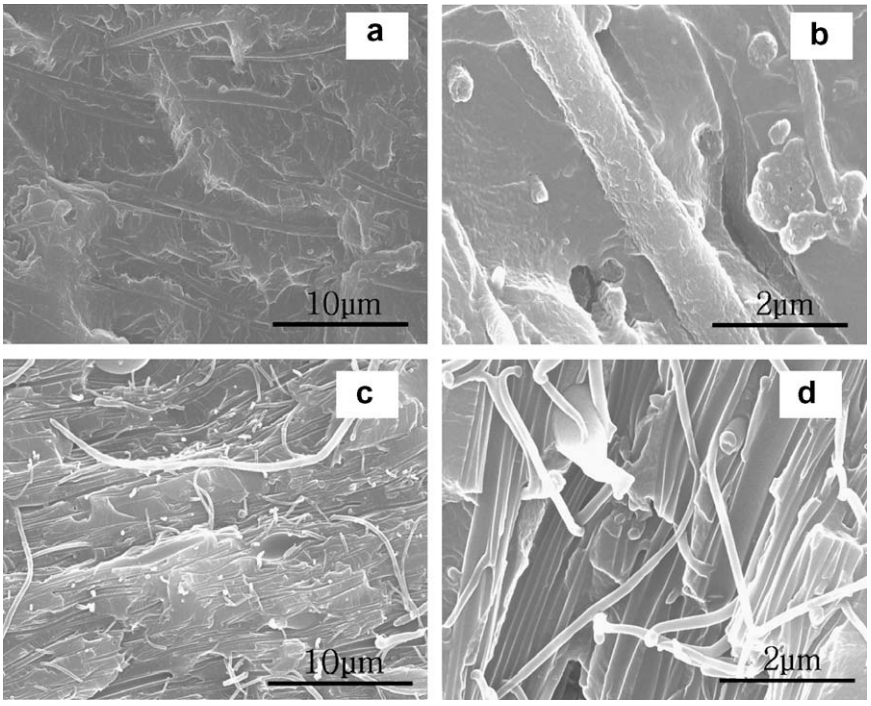

Fig. 5. SEM images of fracture surfaces of three-point flexural testing specimens: composite reinforced with different nanofibers. (a) low magnification of PAN–PMMA nanofibers, (b) high magnification of PAN–PMMA nanofiber, (c) low magnification of PAN nanofiber, (d) high magnification of PAN nanofiber.

composites, but also introduce PAN in the core structure to improve the mechanical properties of the composites. So, this special core–shell structure PAN–PMMA nanofibers reinforced composite should possess strong mechanical properties.

3.3. Dynamic mechanical analysis

The tan δ curves of the composites reinforced with PAN, PMMA and PAN–PMMA nanofibers as a function of temperature are shown in Fig. 7. As shown in Fig. 7(a), for the PMMA nanofiber composites, one broad damping peak is observed for each of the compositions as the PMMA content increases and the damping peak of PMMA nanofiber composites shifts to a higher temperature than that of the neat resin. The literature indicated that only compatible polymers produced an IPN with a broad transition [34]. When two components are mixed in a compatible blend, chain motilities are generally more restrained making the α-transition more difficult and spanning a broader temperature range [34,35]. Therefore, in this study the molecular chain interlock effect between linear PMMA and cross-linked dental resin network was revealed very strongly.

Fig. 7(b) and (c) is the dynamic mechanical properties of the PAN and PAN–PMMA nanofiber reinforced composites. The similar characteristic to the PMMA nanofiber reinforced composites was revealed and the damping peak of both polymers shifted to a higher temperature compared to the neat resin. It is because those nano-reinforcements have been able to affect the segmental motions of the polymer matrix [35,36]. Foremost, impeding chain mobility is possible if the nanofibers are well dispersed in the matrix [37]. But as seen in Fig. 7(c), for the PAN nanofiber composites, there is a tendency to form another damping peak at 100 °C. It was indicated that the composites may have partial phase separation because of the poor interfacial interaction between the PAN nanofibers and the dental resin matrix. In the contrast, for the PAN–PMMA nanofibers, PMMA located in the shell can be dissolved into the resin and then enhance the interface interaction. Therefore, the PAN–PMMA/Bis-GMA composites present single phase morphology as shown in Fig. 7(b).

3.4. Flexural properties

The flexural strength (S_F), flexural modulus (E_Y) and work of fracture (WOF) of the control samples (pure resin without nanofibers) and the dental composites containing 2.5 wt%, 5.0 wt%, 7.5 wt% and 10.0 wt% of electrospun PMMA nanofibers, PAN nanofibers and PAN–PMMA nanofibers reinforced composites, respectively, were measured and the results were shown in Fig. 8. For the PMMA nanofiber reinforced composite, all the S_F, E_Y and WOF values were lower than those of the neat resin. The S_F, E_Y and WOF values were the lowest for the 5 wt% PMMA nanofiber composite, but increased for the 7.5 wt% and 10 wt% PMMA nanofiber composites. Oppositely, the S_F, E_Y and *WOF* of all the PAN and PAN–PMMA nanofiber reinforced composites increased to a certain extent by impregnation of 2.5% mass fractions of the nanofibers. But for PAN nanofiber composite, the mechanical properties decreased remarkably, when the PAN nanofibers increased from 5 wt% to 10 wt%. While for the PAN–PMMA nanofiber composites, the S_F, E_Y and WOF values continuously increased before the mass fraction of the nanofiber increased to 7.5 wt%. Compared to the neat resin, the S_F, E_Y and WOF of the composites reinforced with 7.5% mass fraction of PAN–PMMA nanofibers increased by 18.7%, 14.1% and 64.8%, respectively. But for the composite with 10% mass fraction of PAN–PMMA nanofibers, all the mechanical properties decreased.

Mechanical properties of electrospun nanofibers reinforced composites could be substantially improved by forming a scaffold-like, highly interpenetrated and porous framework [18]. But the small diameter of the nanofibers also provided a high ratio of

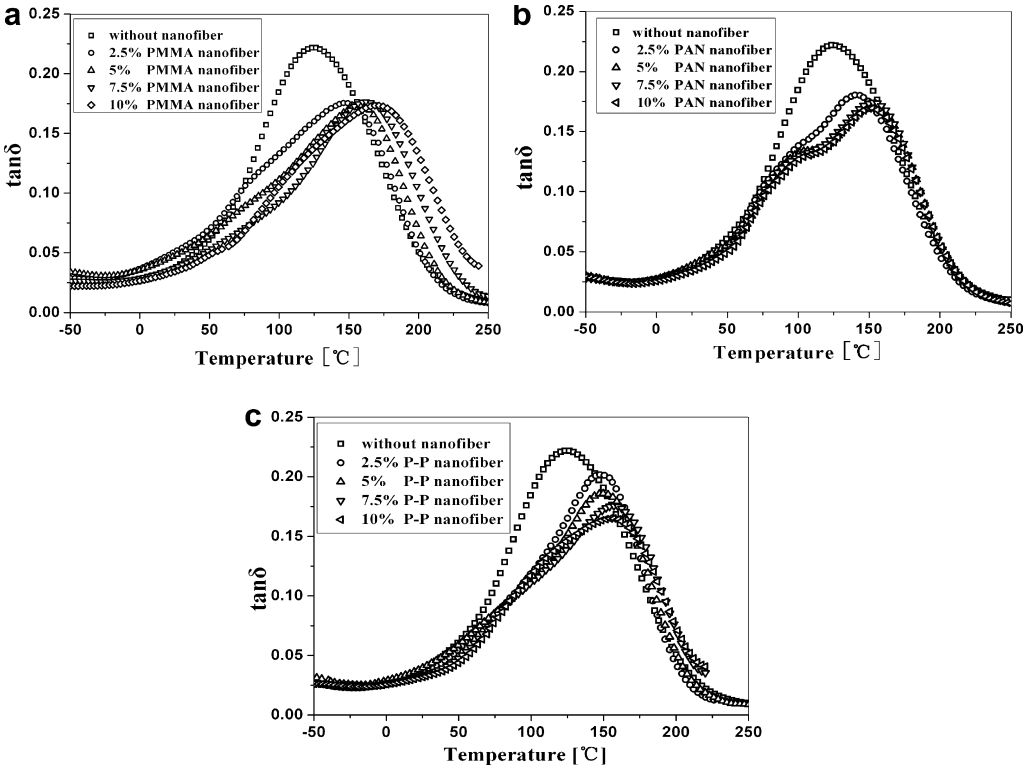

Fig. 7. The tan δ curves of the composites as a function of temperature. (a) PMMA nanofibers, (b) PAN nanofibers, (c) PAN–PMMA nanofibers.

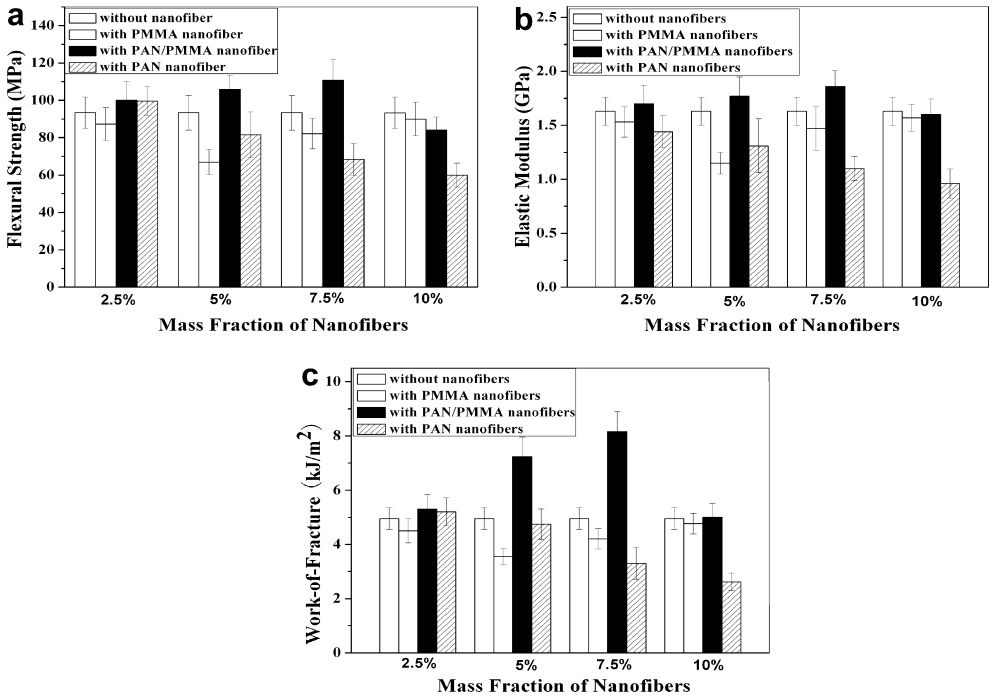

Fig. 8. Mechanical properties of Bis-GMA dental composites reinforced with various mass fractions of nanofibers. (a) Flexural strength, (b) flexural modulus, and (c) work of fracture.

specific area. The more surface area of the nanofibers, the more chance to result in defects (i.e. voids) between nanofibers and dental resin matrix. The further improvements in mechanical properties of the composites via increasing the amount of nanofibers, might be limited by the more defects existing at the interface between the nanofibers and the matrix [18,19]. Therefore, the mechanical properties of the composites were improved simultaneously through the impregnation of small mass fractions of electrospun PAN and PAN–PMMA nanofibers. The frictional force can be created through the pulling out of the nanofibers which were strongly bonded to the dental resin matrix, and the frictional force allowed stress transfer across matrix cracks, and therefore increasing the material resistance to fracture [18]. For the 7.5 wt% nanofibers reinforced composites, the WOF value of the dental composites reinforced with PAN–PMMA nanofibers was much higher than those of the composites reinforced with PAN nanofibers and pure resin (one way analysis of variance (ANOVA), $P > 0{:}05$). This suggested that the special core-shell structure of the PAN–PMMA nanofiber played an important role in improving the interfacial adhesion between the nanofibers and the dental resin matrix.

4. Conclusions

An electrospinning technique of polymer blends was used to fabricate a core-shell structure PAN–PMMA nanofiber in order to reinforce the Bis-GMA dental resin. The PMMA located in the shell could partly be dissolved in dental resin and after photopolymerization, liner PMMA chains interpenetrated and entangled with the crosslinked dental resin network to create an in situ nano-interface in the shell structure with strong interfacial adhesion between nanofibers and matrix. Consequently, the composites present single phase morphology. Compared with the neat resin, the S_F, E_Y and WOF of the composites reinforced with 7.5 wt% mass fraction of PAN–PMMA nanofibers were increased by 18.7%, 14.1% and 64.8%, respectively. Therefore, a new kind of electrospun nanofibers reinforced and toughened composite with strong interfacial bonding between nanofiber and matrix was fabricated. On the basis of this work, many kinds of special core-shell structure of electrospun nanofibers could be designed to reinforce resin by in situ nano-interface formation.

References

[1] Ruddle DE, Maloney MM, Thompson IY. Effect of novel filler particles on the mechanical and wear properties of dental composites. Dent Mater 2002;18(1):72–80.
[2] Xu HHK, Schumacher GE, Eichmiller FC, Peterson RC, Antonucci JM, Mueller HJ. Continuous-fiber preform reinforcement of dental resin composite restorations. Dent Mater 2003;19(6):523–30.
[3] Jandt KD, Al-Jasser AM, Al-Aten K, Vowles RW, Allen GC. Mechanical properties and radiopacity of experimental glass-silica-metal hybrid composites. Dent Mater 2002;18(6):429–35.
[4] Xu HHK. Dental composite resins containing silica-fused ceramic single-crystalline whiskers with various filler levels. J Dent Res 1999;78:1304–11.
[5] Ferracane JL. Correlation between hardness and degree of conversion during the setting reaction of unfilled dental restorative resins. Dent Mater 1985;1(1):11–4.
[6] Li Y, Swartz ML, Phillips RW, Moore BK, Roberts TA. Effect of filler content and size on properties of composites. J Dent Res 1985;64(12):1396–401.
[7] Xu HHK, Martin TA, Antonucci JM, Eichmiller FC. Ceramic whisker reinforcement of dental composite resins. J Dent Res 1999;78(2):706–12.
[8] Schaefer DW, Justice RS. How nano are nanocomposites? Macromolecules 2007;40(24):8501–17.
[9] Zhao F, Takeda N. Effect of interfacial adhesion and statistical fiber strength on tensile strength of unidirectional glass fiber/epoxy composites. Part I: experimental results. Composites A 2000;31:1203–14.
[10] Kessler A, Bleddzki A. Correlation between interphase-relevant tests and the impact-damage resistance of glass/epoxy laminates with different fibre surface treatments. Compos Sci Technol 2000;60(1):125–30.
[11] Debnath S, Ranadea R, Wunder SL. Interface effects on mechanical properties of particle-reinforced composites. Dent Mater 2004;20(7):677–86.
[12] Gao J, Zhao B, Itkis ME, Bekyarova E. Chemical engineering of the single-walled carbon nanotube-nylon 6 interface. J. Am. Chem. Soc 2006;128(23):7492–6.
[13] Yoshida Y, Shirai K, Nakayama Y, Itoh M, Okazaki M. Improved filler–matrix coupling in resin composites. J Dent Res 2002;81:270–3.
[14] Tian M, Gao Y, Liu Y. Fabrication and evaluation of Bis-GMA/TEGDMA dental resins/composites containing nano fibrillar silicate. Dent Mater 2008;24(2):235–43.
[15] Ericksona RL, Davidsonb CL, Halvorsona RH. The effect of filler and silane content on conversion of resin-based composite. Dent Mater 2003;19(4):327–33.
[16] Craig RG, Powers JM. Restorative dental materials. 11th ed. Mosby: St Louis; 2002.

[17] Zandinejada AA, Pahlevana MA. The effect of ceramic and porous fillers on the mechanical properties of experimental dental composites. Den Mater 2006;22(4):382–7.
[18] Fong H. Electrospun nylon 6 nanofiber reinforced BIS-GMA/TEGDMA dental restorative composite resins. Polymer 2004;45(7):2427–32.
[19] Tian M, Gao Y, Liu Y. Bis-GMA/TEGDMA dental composites reinforced with electrospun nylon 6 nanocomposite nanofibers containing highly aligned fibrillar silicate single crystals. Polymer 2007;48(9):2720–8.
[20] Jong-Sang Kim, Darrell H, Reneker. Mechanical properties of composites using ultrafine electrospun fibers. Polym Compos 1999;20:124–31.
[21] Bergshoef MM, Vancso GJ. Transparent nanocomposites with ultrathin, electrospun Nylon-4,6 fiber reinforcement. Adv Mater 1999;11:1362–5.
[22] Sun Z, Zussman E, Yarin AL, Wendorff JH, Greiner A. Compound core–shell polymer nanofibers by co-electrospinning. Adv Mater 2003;15(22):1929–32.
[23] Bazilevsky AV, Yarin AL, Megaridis CM. Co-electrospinning of core-shell fibers using a single-nozzle technique. Langmuir 2007;23(5):2311–4.
[24] Wei M, Lee J, Kang B, Mead J. Preparation of core–sheath nanofibers from conducting polymer blends. Macromol Rapid Commun 2005;26(14):1127–32.
[25] Zussman E, Yarin AL, Bazilevsky AV, Avrahami R, Feldman M. Electrospun polyacrylonitrile/poly(methyl methacrylate)-derived turbostratic carbon micro-/nanotubes. Adv Mater 2006;18:348–53.
[26] Chen LS, Huang ZM, Dong GH, He CL, Liu L, Hu YY, et al. Development of a transparent PMMA composite reinforced with nanofibers. Polym Compos. 2008. 10.1002/pc.20551 (Published online in Wiley InterScience (www.interscience.wiley.com)).
[27] Lastumäki TM, Lassila LVJ, Vallittu PK. The semi-interpenetrating polymer network matrix of fiber-reinforced composite and its effect on the surface adhesive properties. Mater Sci Mater Med 2003;14(9):803–9.
[28] Garoushi S, Vallittu PK, Lassila LVJ. Short glass fiber reinforced restorative composite resin with semi-inter penetrating polymer network matrix. Dent Mater 2007;23(11):1356–62.
[29] Li G, Li P, Yang XP. Inhomogeneous toughening of carbon fiber/epoxy composite using electrospun polysulfone nanofibrous membranes by in situ phase separation. Compos Sci Tech 2008;68(3-4):987–94.
[30] Wei M, Kang B, Sung C. Core–sheath structure in electrospun nanofibers from polymer blends. Macromol Mater Eng 2006;291(11):1307–14.
[31] Tannenbaum R, Zubris M, David K. FTIR characterization of the reactive interface of cobalt oxide nanoparticles embedded in polymeric matrices. J Phys Chem B 2006;110(5):2227–32.
[32] Ciprari D, Jacob K, Tannenbaum R. Characterization of polymer nanocomposite interphase and its impact on mechanical properties. Macromolecules 2006;39(19):6565–73.
[33] Seo Y, Lee J, Kang TJ, Choi HJ, Kim J. In situ compatibilizer reinforced interface between an amorphous polymer (polystyrene) and a semicrystalline polymer (polyamide nylon 6). Macromolecules 2007;40(16):5953–8.
[34] Rong MZ, Zeng HM. Polycarbonate-epoxy semi-interpenetrating polymer network: 2. Phase separation and morphology. Polymer 1997;38(2):269–77.
[35] Petersson L, Oksman K. Biopolymer based nanocomposites: comparing layered silicates and microcrystalline cellulose as nanoreinforcement. Compos Sci Tech 2006;66(13):2187–96.
[36] Subramani S, Lee JY, Kim JH. Crosslinked aqueous dispersion of silylated poly (urethane–urea)/clay nanocomposites. Compos Sci Tech 2007;67(7):1561–73.
[37] Khaled SM, Sui R, Charpentier PA. Synthesis of TiO_2–PMMA nanocomposite: using methacrylic acid as a coupling agent. Langmuir 2007;23(7):3988–95.